Magnetic Enhancement of γ-Fe 2 O 3 Nanoparticles by Sonochemical Coating

10 AUTHORS, INCLUDING:

Abraham Ulman
Polytechnic Institute of New York University
93 PUBLICATIONS 11,859 CITATIONS

SEE PROFILE

Xingzhong Yan
Texas A&M University - Commerce
76 PUBLICATIONS 1,140 CITATIONS

SEE PROFILE

Claude Estournès
Inter-university Material Research and Engin…
220 PUBLICATIONS 3,636 CITATIONS

SEE PROFILE

Miriam Rafailovich
Stony Brook University
227 PUBLICATIONS 3,058 CITATIONS

SEE PROFILE

Magnetic Enhancement of γ-Fe₂O₃ Nanoparticles by Sonochemical Coating

Kurikka V. P. M. Shafi,[†,‡] Abraham Ulman,*,[†,‡] Ansil Dyal,[†,‡] Xingzhong Yan,[‡,§]
Nan-Loh Yang,[‡,§] Claude Estournès,[||] Léopold Fournès,[⊥] Alain Wattiaux,[⊥]
Henry White,[‡,#] and Miriam Rafailovich[‡,#]

*Department of Chemical Engineering and Chemistry, Polytechnic University,
Brooklyn, New York 11201, Department of Chemistry, CUNY at Staten Island,
2800 Victory Boulevard, Staten Island, New York 10314, The NSF MRSEC for Polymers at
Engineered Interfaces, Institut de Physique et Chimie des Matériaux de Strasbourg, Groupe
des Matériaux Inorganiques, 23 rue du Loess, 67037 Strasbourg Cedex, France, Institut de
Chimie de la Matière Condensée de Bordeaux, 87 Avenue du Docteur Schweitzer,
33608 Pessac Cedex, France, and Department of Materials Sciences and Engineering, State
University of New York at Stony Brook, Stony Brook, New York 11794-2275*

We show that sonochemistry is an efficient and facile route for quantitative coating of γ-Fe₂O₃ nanoparticles with octadecyltrihydrosilane (OTHS, $CH_3(CH_2)_{17}SiH_3$). The presence of C−H stretching (2950−2850 cm⁻¹) and bending (1475−1375 cm⁻¹) bands, and the absence of peaks at 2150 and 925 cm⁻¹ (Si−H stretching and bending respectively) confirm the presence of grafted hydrocarbon chains in the irradiated sample, hence the reaction of OTHS with γ-Fe₂O₃ nanoparticles. The coated nanoparticles show increased magnetization compared to the uncoated ones. X-ray diffraction, magnetization studies, Mössbauer spectra, and electron paramagnetic resonance spectra reveal that the magnetic ordering is more prominent in the OTHS-coated γ-Fe₂O₃ sample because of improved crystallinity.

Introduction

Nanoparticles have become the focus of modern materials science because of their potential technological importance, which stems from their unique physical properties.[1] These properties result from their reduced dimensions: for example, semiconductor nanoparticles (quantum dots) exhibit discrete energy bands and size-dependent band gap energies; conducting nanoparticles exhibit large optical polarizabilities and nonlinear electrical conductance; superconductor nanoparticles exhibit a size-dependent transition temperature; and ferromagnetic nanoparticles become superparamagnetic (spm), with size-dependent magnetic susceptibilities.[2] However, studies on magnetic nanoparticles of these dimensions are scanty compared to, say, those on nanosized semiconductor particles. Magnetic nanoparticles have

applications in information storage,[3] in color imaging,[4] in magnetic refrigeration,[5] in bioprocessing,[6] in medical diagnosis,[7] in controlled drug delivery,[8] and as ferrofluids.[9] Thus, developing a new synthetic route for these particles and the investigation of their properties are of great importance.

Various methods have been reported for the synthesis of iron oxide nanoparticles, such as wet chemical,[10] electrochemical,[11] and pyrolysis[12] techniques, and chemical oxidation in micellar media[13] or in polymer[14] or mineral matrices.[15] In general, these methods do not

* To whom correspondence should be addressed. Phone: (718) 260-3119. Fax: (718) 260-3125. E-fax: (810) 277-6217. E-mail: aulman@poly.edu.
† Polytechnic University.
‡ The NSF MRSEC for Polymers at Engineered Interfaces.
§ CUNY at Staten Island.
|| Institut de Physique et Chimie des Matériaux de Strasbourg.
⊥ Institut de Chimie de la Matière Condensée de Bordeaux.
State University of New York at Stony Brook.

(1) (a) Ozin, G. A. *Adv. Mater.* **1992**, *4*, 612. (b) Gleiter, H. *Adv. Mater.* **1992**, *4*, 474.
(2) (a) Brus, L. E.; et al. *J. Mater. Res.* **1989**, *4*, 704. (b) *Nanostructures and Quantum Effects*; Sakaki, H., Noge, H., Eds.; Springer-Verlag: Berlin, 1994. (c) Woggon, U. *Optical Properties of Semiconductor Quantum*; Springer-Verlag: Berlin, 1997. (d) *Nanomagnetism*; Hernando, A., Ed.; Kluwer Academic Publishers: Dordrecht, The Netherlands, 1993. (e) *Magnetic Properties of Fine Particles*; Dormann, J. L., Fiorani, D., Eds.; North-Holland: Amsterdam, 1992. (f) *Science and Technology of Nanostructured Magnetic Materials*; Hadjipanayis, G. C., Prinz, G. A., Eds.; Plenum Press: New York, 1991.

(3) Audram, R. G.; Huguenard, A. P. U.S. Patent 4302523, 1981.
(4) Ziolo, R. F. U.S. Patent 4474866, 1984.
(5) McMichael, R. D.; Shull, R. D.; Swartzendruber, L. J.; Bennett, L. H.; Watson, R. E. *J. Magn. Magn. Mater.* **1992**, *111*, 29.
(6) Pope, N. M.; Alsop, R. C.; Chang, Y.-A.; Sonith, A. K. *J. Biomed. Mater. Res.* **1994**, *28*, 449.
(7) (a) Marchessault, R. H.; Richard, S.; Rioux, P. *Carbohydr. Res.* **1992**, *224*, 133. (b) Josephson, L.; Tsung, C. H.; Moore, A.; Weissleder, R. *Bioconjugate Chem.* **1999**, *10*, 186.
(8) Bhatnagar, S. P.; Rosensweig, R. E. *J. Magn. Magn. Mater.* **1995**, *149*, 198.
(9) Rosensweig, R. E. *Ferrohydrodynamics*; MIT Press: Cambridge, MA, 1985.
(10) (a) Kang, Y. S.; Risbud, S.; Rabolt, J. F.; Stroeve, P. *Chem. Mater.* **1996**, *8*, 2209. (b) Ennas, G.; Marangiu, G.; Musinu, A.; Falqui, A.; Ballirano, P.; Caminiti, R. *J. Mater. Res.* **1999**, *14*, 1570.
(11) Pascal, C.; Pascal, J. L.; Favier, F.; Moubtassim, M. L. E.; Payen, C. *Chem. Mater.* **1999**, *11*, 141.
(12) (a) Martinez, B.; Roig, A.; Molins, E.; Gonzalez-Carreno, T.; Serna, C. J. *J. Appl. Phys.* **1998**, *83*, 3256. (b) Morale, M. P.; Veintemillas-Verdaguer, S.; Serna, C. J. *J. Mater. Res.* **1999**, *14*, 3066.
(13) Mounien, N.; Pileni, M. P. *Langmuir* **1997**, *13*, 3927.
(14) (a) Ziolo, R.; Giannelis, E. P.; Weinstein, B. A.; O'Horo, M. P.; Ganguly, B. N.; Mehrotra, V.; Russel, M. W.; Huffman, D. R. *Science* **1992**, *257*, 219. (b) Tang, B. Z.; Geng, Y.; Lam, J. W. Y.; Li, B.; Jing, X.; Wang, X.; Wang, F.; Pakhomov, A. B.; Zhang, X. X. *Chem. Mater.* **1999**, *11*, 1581.

yield pure amorphous phases, and good control of particles size, and achieving monodispersity (i.e., narrow size distribution) are still the challenge in all these techniques.

In sonochemistry, the acoustic cavitation, that is, the formation, growth, and implosive collapse of a bubble in an irradiated liquid, generates a transient localized hot spot, with an effective temperature of 5000 K and a nanosecond lifetime.[16] This process has been used to prepare various kinds of nanostructured amorphous magnetic materials of metals,[17] metal alloys,[18] oxides,[19] ferrites,[20] and nitrides.[21] The advantage of sonochemistry is that one can obtain atomic level mixing of the constituent species in the amorphous phase so that the crystalline phase can be obtained by annealing at relatively low temperatures. The rapid cavitational cooling ($\geq 10^{10}$ K s^{-1}) can be viewed as a quenching process; hence, the composition of the particles formed should be identical to the composition of the vapor in the bubbles, without phase separation. This should allow, in principle, the preparation of materials with unusual and unique compositions that might have novel properties.

Maghemite (γ-Fe₂O₃, the ferrimagnetic cubic form of iron(III) oxide) is technologically important, as it is being used widely for the production of magnetic materials and catalysts. Because of the small coercivity of Fe₂O₃ nanoparticles, which arises from a negligible barrier in the hysteresis of the magnetization loop, they can be used as magneto-optical devices. Magneto-optic media can be made by depositing magnetic and optically transparent materials, and maghemite particles satisfy this condition, since they can be easily incorporated into ultrathin polymer films.[14,22] Our interest is the preparation, functionalization, and exploitation of nanoparticles, both as nanodevices, using insights from biology, and as building blocks for advanced metamaterials, exploiting "small" scale physics, using the traditional disciplines of chemistry and polymer science. This requires development of facile, efficient, and preferably quantitative surface functionalization reactions and chemistries (such as those that follow), to allow the attachment of functional molecular and macromolecular moieties. In addition, the incorporation of nanoparticles within organic matrices requires surface functionalization to prevent phase separation and aggregation.

Coating of amorphous Fe₂O₃ nanoparticles with surfactants can be accomplished by simply mixing with the surfactant solution. This way, amorphous Fe₂O₃ nano-

particles were coated with a monolayer of thiols,[23] alcohols,[24] carboxylic acids,[25] octadecyltrichlorosilane (OTS), and sodium dodecyl sulfate (SDS).[26] However, when amorphous Fe₂O₃ nanoparticles are converted to the pure γ-Fe₂O₃ phase, by heating at 300 °C for 3 h, the crystalline nanoparticles cannot be functionalized easily, even after prolonged exposure to the surfactant solutions. The coating of γ-Fe₂O₃ nanoparticles by bolaamphiphiles has been reported previously.[27,28] Liu and co-workers have reported a two-step silica-coating process, a sol-gel method followed by dense liquid coating.[29] Though this method gives a complete coverage, the experiment is laborious. In this paper, we report that sonicating γ-Fe₂O₃ nanoparticles with octadecyltrihydrosilane (OTHS, $CH_3(CH_2)_{17}SiH_3$) in heptane results in their facile and efficient coating, and also in the enhancement of their magnetic properties.

Experimental Section

Amorphous Fe₂O₃ nanoparticles were prepared[30] by ultrasonic decomposition of the volatile precursor (Fe(CO)₅) (Aldrich) solution in anhydrous decane. Thus, a decane solution of 0.5 M Fe(CO)₅ was sonicated at 273 K for 3 h under air atmosphere, using a high-intensity ultrasonic probe (Sonics, Model VC 601, 1.25 cm Ti horn, 20 kHz, 100 W/cm²). The resulting black solution was then centrifuged (9000 rpm, 5 min, 10 °C) and washed with anhydrous pentane. Centrifugation and washing were repeated at least five times to remove the excess Fe(CO)₅ and the possible byproducts, and the product was then dried under vacuum.

γ-Fe₂O₃ nanoparticles were prepared by annealing the as-prepared amorphous particles at 300 °C for 180 min in a furnace under air atmosphere.

OTHS-coated γ-Fe₂O₃ nanoparticles were prepared by ultrasonic irradiation of the slurry of the γ-Fe₂O₃ nanoparticles in an anhydrous heptane solution of OTHS (Aldrich) at 273 K with a high-intensity ultrasonic probe. After 10 min of irradiation, a suspension was obtained which was then centrifuged (9000 rpm, 5 min, 10 °C) and washed with anhydrous pentane. Centrifugation and washing were repeated at least five times to ensure the complete removal the OTHS excess. The product was then dried under vacuum. The irradiation process was repeated for 30 min and for 1, 2, and 3 h, respectively.

Transmission electron microscopy (TEM) measurements were carried out by placing one or two drops of suspension in hexane onto a carbon stabilized Formvar-coated copper grid (200 mesh) and drying it.

Powder X-ray diffractograms were recorded on a Philips X-ray diffractometer (Cu Kα radiation, $\lambda = 1.5418$ Å).

Fourier transform infrared (FTIR) spectra of the particles were recorded on a Nicolet 760 spectrophotometer equipped with a He−Ne laser and an MCT detector, at 2 cm^{-1} resolution. The samples were prepared by mixing the nanoparticles with spectroscopic grade KBr in the ratio 1:50.

Magnetic data of the solid samples were obtained with a Princeton Applied Research vibrating sample magnetometer

(15) (a) del Monte, F.; Morale, M. P.; Levy, D.; Fernandez, A.; Ocana, M.; Roig, A.; Molins, E.; O'Grady, K.; Serna, C. J. *Langmuir* **1997**, *13*, 3627. (b) Froba, M.; Kohn, R.; Bouffard, G. *Chem. Mater.* **1999**, *11*, 2858.

(16) (a) Suslick, K. S. *Science* **1990**, *247*, 1439. (b) Flint, E. B.; Suslick, K. S. *Science* **1991**, *253*, 1397. (c) Atchley, A. A.; Crum, L. A. In *Ultrasound, its Chemical, Physical and Biological Effect*; Suslick, K. S., Ed.; VCH Press: New York, 1988.

(17) Koltypin, Yu.; Katabi, G.; Cao, X.; Prozorov, R.; Gedanken, A. *J. Non-Cryst. Solids* **1996**, *201*, 159.

(18) Shafi, K. V. P. M.; Gedanken, A.; Goldfarb, R. B.; Felner, I. *J. Appl. Phys.* **1997**, *81*, 6901.

(19) Cao, X.; Koltypin, Yu.; Prozorov, R.; Felner, I.; Gedanken, A. *J. Mater. Chem.* **1997**, *7*, 1007.

(20) Shafi, K. V. P. M.; Gedanken, A.; Prozorov, R.; Balogh, J. *Chem. Mater.* **1998**, *10*, 3445.

(21) Koltypin, Yu.; Cao, X.; Prozorov, R.; Balogh, J.; Kaptas, D.; Gedanken, A. *J. Mater. Chem.* **1997**, *7*, 2453.

(22) Kang, Y. S.; Risbud, S.; Rabolt, J. F.; Stroev, P. *Chem. Mater.* **1996**, *8*, 2209.

(23) Kataby, G.; Prozorov, T.; Koltypin, Yu.; Sukenik, C. N.; Ulman, A.; Gedanken, A. *Langmuir* **1997**, *13*, 6151.

(24) Kataby, G.; Ulman, A.; Prozorov, R.; Gedanken, A. *Langmuir* **1998**, *14*, 1512.

(25) Kataby, G.; Cojocaru, M.; Prozorov, R.; Gedanken, A. *Langmuir* **1999**, *15*, 1703.

(26) Rozenfeld, O.; Koltypin, Y.; Bamnolker, H.; Margel, S.; Gedanken, A. *Langmuir* **1994**, *10*, 627.

(27) Liu, Q.; Xu, Z. *J. Appl. Phys.* **1996**, *79*, 4702.

(28) Gelina, S.; Finch, J. A.; Bohme, P. *Colloids Surf.* **2000**, *172*, 103.

(29) Liu, Q.; Xu, Z.; Finch, J. A.; Egerton, R. *Chem. Mater.* **1998**, *10*, 3936.

(30) Shafi, K. V. P. M.; Ulman, A.; Yan, X.; Yang, N.-L.; Estournes, C.; White, H.; Rafailovich, M. *Langmuir* **2001**, *17*, 5093.
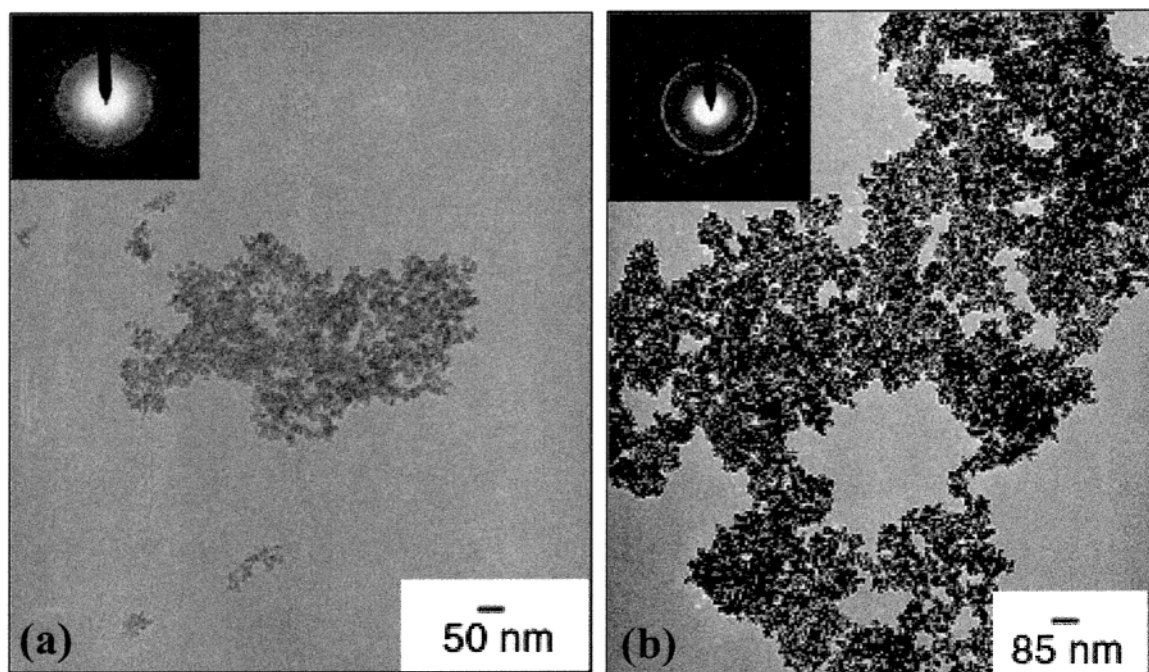
Figure 1. TEM micrographs of γ-Fe$_2$O$_3$ crystalline nanoparticles before (a) and after coating with OTHS (b).

model 155 (VSM) and a Quantum Design SQUID MPMS-XL (ac and dc modes and maximum static field of ±5 T).

EPR spectra were recorded in the X-band on a Bruker ESP380E spectrometer equipped with a HP5361 frequency counter and a variable-temperature accessory, BVT-2000 system. The spectra for *g*-value and spin density calculations were obtained at room temperature using the following parameters: microwave power, 0.72–0.73 mW; modulation amplitude, 1.0 G; modulation frequency, 100 kHz; time constant, 1.28 ms; sweep time, up to 168 s; sweep width, 3600 G; *X* axis resolution, 4 K. Spin density was estimated on the basis of the intensity of the DPPH (2.26 × 10^{15} spins) as an internal standard marker calibrated against Mn^{2+}/CaO with a known spin number. Sample in a 5 mm i.d. NMR tube was kept at the desired temperature for 15–20 min to allow thermal equilibrium. No saturation was found at the microwave power 0.73–0.74 mW in the variable temperature range.

Mössbauer measurements were performed using a constant acceleration HALDER-type spectrometer with a room-temperature ^{57}Co source (Rh matrix) in transmission geometry. The polycrystalline absorbers containing about 10 mg cm^{-2} of iron were used to avoid the experimental widening of the peaks. The spectra at 4.2 and 293 K were recorded using a variable-temperature cryostat. The velocity was calibrated using pure iron metal as the standard material. The refinement of the Mössbauer spectra showed an important and abnormal widening of the peaks, so that the spectra have been fitted assuming a distribution either of quadrupolar splittings or of hyperfine fields.

Thermal Analysis. The samples were heated to 900 °C at a rate of 10 deg/min, under a nitrogen atmosphere on a TA 2950 Hi Res. TGA.

Results and Discussion

Figure 1 presents images of γ-Fe$_2$O$_3$ nanoparticles before and after coating with OTHS, respectively. The images shown are with the maximum magnification within the instrumental limit. The SAED pattern indicates the nanocrystallinity, and the image shows the γ-Fe$_2$O$_3$ particles are agglomerates of small particles with overall diameters < 25 nm. Most of the particles are aggregated, so it is difficult to determine the exact shape. The aggregation of the particles is inherent in

the sonochemical technique, since the high velocity of interparticle collisions during the irradiation causes the particle to coalesce. A closer look at the nanodiffraction patterns reveals that crystallinity increases after coating, as the pattern becomes much more clear and has more spots. This is further evidenced from the X-ray analysis shown later.

Figure 2 shows infrared spectra of γ-Fe$_2$O$_3$ before (Figure 2b) and after sonication with OTHS for 3 h (Figure 2a). The broad band at 3400–3500 cm^{-1} shows the presence of surface hydroxyls. The presence of C–H stretching (2950–2850 cm^{-1}) and bending (1475–1375 cm^{-1}) bands, and the absence of peaks at 2150 and 925 cm^{-1} (Si–H stretching and bending, respectively; Figure 2c) confirm the presence of grafted hydrocarbon chains in the irradiated sample, hence the reaction of OTHS with γ-Fe$_2$O$_3$ nanoparticles. The broad band at 1000–1200 cm^{-1}, which can be inferred to be caused by the presence of Fe–O–Si, Si–O–Si, and Fe–O–Fe species, provides further evidence for surface attachment of octadecyl chains. Longer sonication time did not result in observable differences in the FTIR spectra, and samples irradiated for 30 min and for 3 h had identical spectra. This suggests that the coating reaction is complete within 30 min of the irradiation time.

This is further supported by the weight loss measurements of thermogravimetric analysis curves of the γ-Fe$_2$O$_3$ nanoparticles before (Figure 3) and after sonication with OTHS for various periods of time. The mass loss, as well as the high desorption temperature, confirms strong binding between the surfactant molecules and the γ-Fe$_2$O$_3$ particles. The thermograms of the 30 min to 3 h irradiated samples show nearly the same weight loss, corroborating that the reaction is complete within 30 min of ultrasound exposure. The total weight loss of the silane-coated γ-Fe$_2$O$_3$ samples of 13–14% indicates, after accounting for the weight loss for uncoated γ-Fe$_2$O$_3$ particles (~4%), a full surface coverage of γ-Fe$_2$O$_3$ particles of average 25 nm in size.
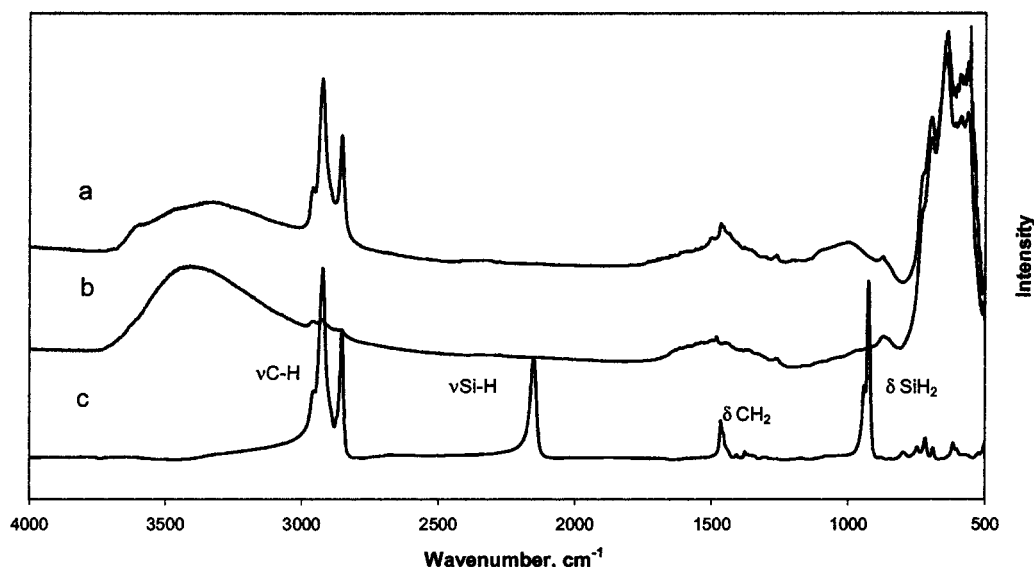
Figure 2. FTIR spectra of γ-Fe$_2$O$_3$ crystalline nanoparticles before (b) and after coating with OTHS for 3 h (a). Part c shows the spectrum of OTHS.
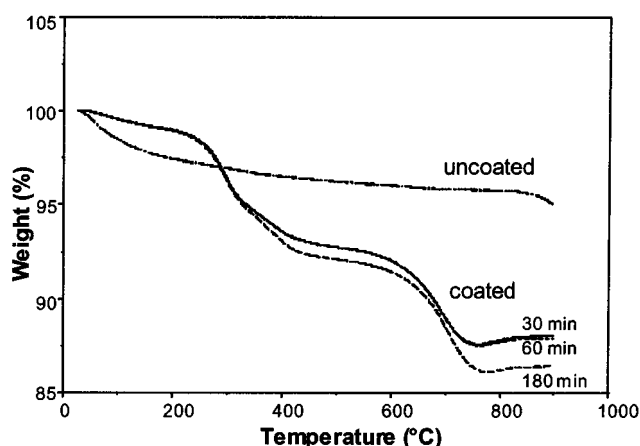

Figure 3. Weight loss analysis from TGA curves of γ-Fe$_2$O$_3$ crystalline nanoparticles before and after coating with OTHS for various periods of time ($10 \leq t \leq 180$ min).

Figure 4. Room-temperature magnetization curves of the as-prepared amorphous, heated crystalline, and OTHS-coated nanoparticles of γ-Fe$_2$O$_3$ for various periods of time ($10 \leq t \leq 180$ min).

The early weight loss until 200 °C of the uncoated γ-Fe$_2$O$_3$ particles is probably due to the removal of surface hydroxyls and/or surface adsorbed water, as is evident from the strong OH bands in the IR spectrum of the uncoated γ-Fe$_2$O$_3$. Notice this early loss is minimal and the intensity of the OH band is less compared to that for the coated one, confirming the reaction of the silane molecule with the surface hydroxyls. The Fe–OH bond reacts with the Si–H bonds of the silane, giving Fe–O–Si species with the elimination of the H$_2$ molecule, similar to the surface reaction reported previously for titania surfaces by Fadeev and McCarthy[31] and for titania nanoparticles by our group.[32]

Room-temperature magnetization curves of the amorphous (Am-FeO) as well as the heated crystalline γ-Fe$_2$O$_3$ nanoparticles before (Cr-FeO) and after a sonication with OTHS (Cr-FeOSil) for various irradiation time periods ($10 \leq t \leq 180$ min) are shown in Figure 4. Notice that the measurements were carried out on
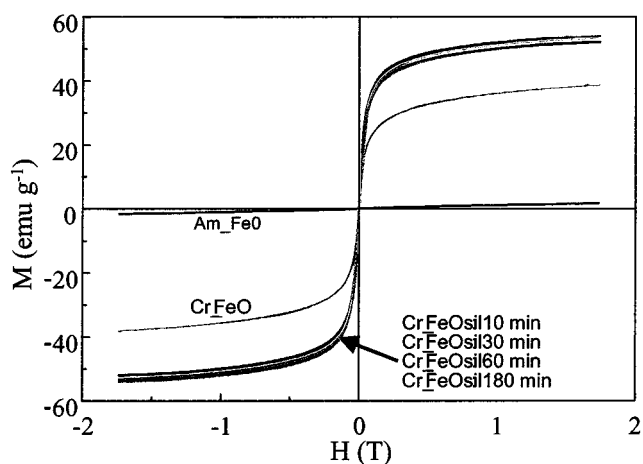
(31) Fadeev, A. Y.; McCarthy, T. J. *J. Am. Chem. Soc.* **1999**, *121*, 12184.

(32) Shafi, K. V. P. M.; Ulman, A.; Yan, X.; Yang, N.-L.; Himmelhaus, M.; Grunze, M. *Langmuir* **2001**, *17*, 1726.
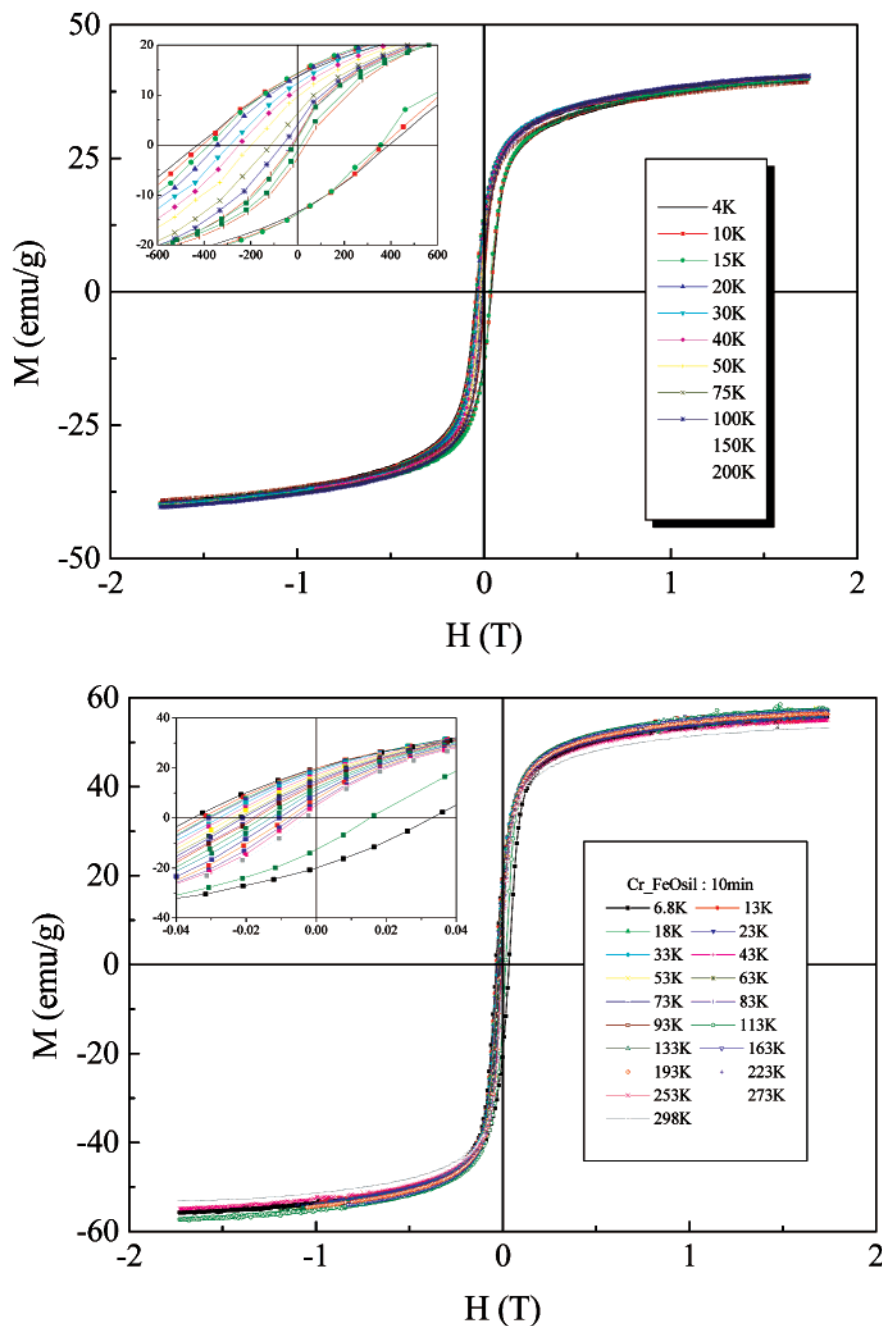
uncoated samples of γ-Fe$_2$O$_3$ nanoparticles that were sonicated for 3 h in heptane in the absence of OTHS to ensure that samples had the same treatment history. The amorphous Fe$_2$O$_3$ sample (Am-FeO) behaves as expected, showing a very low magnetization value with the curve not reaching saturation and no hysteresis, which is characteristic of superparamagnetic (spm) nanoparticles with size less than 10 nm.

The observed saturation magnetization value of the crystalline Fe$_2$O$_3$ nanoparticles before coating is about 35 emu g^{-1}, which is significantly lower than that for the reported multidomain bulk particles (74 emu g^{-1}).[14] The difference in magnetization value between bulk and our nanoparticles can be attributed to the small particle size effect. It is known that magnetic properties, that is, the saturation magnetization and hyperfine field value, of nanoparticles are much smaller than those of the corresponding bulk materials.[12,13,33] γ-Ferrite, γ-Fe$_2$O$_3$, is a spinel-type collinear ferrimagnetic spin structure in the bulk form. The decrease in the saturation magnetization in 10–100 nm nanoparticles has been explained in terms of noncollinear spin arrange-

Figure 5. Variable-temperature magnetization curves of the heated crystalline (a, top) (Cr_FeO) and OTHS-coated (b, bottom) (Cr_FeOsil: 10 min) γ-Fe$_2$O$_3$ nanoparticles. The inset shows the hysteresis loops.

ment at or near the surface of the particle.[34,35] Such a noncollinear structure, which is attributed to a surface effect, is more pronounced in small particle sizes such as in our sample. It was found that, for microcrystalline γ-Fe$_2$O$_3$ particles of about 100 nm in size, the degree of order in cation vacancies, which is inherent to the γ-Fe$_2$O$_3$ structure, affects the magnetic properties.[36] Another study showed that, for γ-Fe$_2$O$_3$ nanoparticles, cation ordering is only observed for particles larger than 20 nm.[37] Therefore, the cation disorder together with the magnetically disordered surface layer around the particles could be the reason for the observed low saturation magnetization. The presence of amorphous impurities on the surface can also reduce the total magnetization. The disordered spins in the amorphous system lead to a dispersion in the exchange constant, which can suppress the magnetic moment. Finally, the small quantities of nonmagnetic organic impurities and antiferromagnetic oxide or carbide impurities can also

(33) (a) Shafi, K. V. P. M.; Koltypin, Y.; Gedanken, A.; Prozorov, R.; Balogh, J.; Lendvai, J.; Felner, I. *J. Phys. Chem.* **1997**, *101*, 6409. (b) Moumen, N.; Pileni, M. P. *J. Phys. Chem.* **1996**, *100*, 1867. (c) Cullity, B. D. *Introduction to Magnetic Materials*; Addison-Wesley: Reading, MA, 1972. (d) Craik, D. J. *Magnetic Oxides*; Wiley: New York, 1975; Part 2, pp 697−708. (e) Greenwood, N. N.; Gibb, T. C. *Mössbauer Spectroscopy*; Chapman and Hall: London, 1971.
(34) (a) Haneda, K.; Morrish, A. H. *J. Appl. Phys.* **1988**, *63*, 4258. (b) Morales, M. P.; Verdaguer, S. V.; Montero, M. I.; Serna, C. J.; Roig, A.; Casas, L.; Martinez, B.; Sandiumenge, F. *Chem. Mater.* **1999**, *11*, 3058.
(35) Morup, S.; Bodker, F.; Hendriksen, P. V.; Linderoth, S. *Phys. Rev B* **1995**, *52*, 287.

(36) Morales, M. P.; Serna, C. J.; Bodger, F.; Morup, S. J. *J. Phys.: Condens. Matter* **1997**, *9*, 5461.
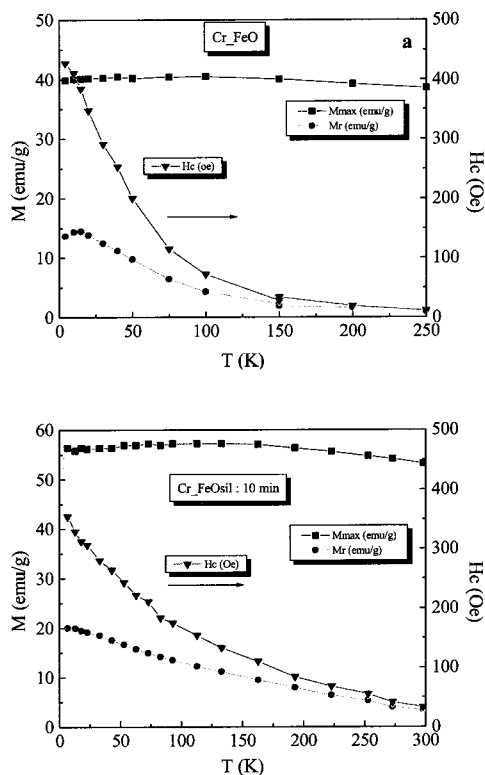(37) Haneda, K.; Morrish, A. H. *Solid State Commun.* **1977**, *22*, 779.

Figure 6. Temperature dependence of the magnetization, remanence, and coercivity for the crystalline γ-Fe₂O₃ nanoparticles before (Cr_FeO, a) and after coating with OTHS (Cr_FeOsil: 10 min, b). The inset shows the hysteresis loops.

reduce the total magnetization. Interestingly, the sonochemical coating with OTHS results in a significant increase in magnetization (55 emu g^{-1}). Parts a and b of Figure 5 present variable-temperature magnetization loops for the γ-Fe₂O₃ nanoparticles before and after coating with OTHS, respectively. Figure 6 presents plots of magnetic coercivity and remanence at various temperatures for the same samples.

The magnetic enhancement of the γ-Fe₂O₃ nanoparticles after sonochemical coating with OTHS is evident at all temperatures. The silane-coated particles show high magnetic saturation and remanence values at all temperatures, exhibiting more ferromagnetic ordering than the uncoated particles. The reduced remanence (ratio of remanence to saturation) and coercivity at 4.2 K are almost equal in both coated and uncoated nanoparticles. The extrapolated reduced remanence, $M_r(0)/M_s(0)$, values are 0.36 and 0.35, and the coercivity $H_c(0)$ values are 425 and 375 Oe for coated and uncoated nanoparticles, respectively.

For noninteracting particles with uniaxial anisotropy, $M_r(0)/M_s(0) = 0.5$. However, for interacting particles, as in the powder sample where interparticle separation is small, the extrapolated remanence is expected to be lower because of more or less complete flux closure[35,38] and the values are comparable to those reported, that is, 0.33 and 0.32, respectively, for oleic acid coated and uncoated dried maghemite powder samples, prepared by the wet chemical method.[35] The low-temperature coercive fields of the two samples, coated and uncoated particles, are not appreciably larger than expected (75

(38) Bean, C. P.; Livingston, J. D. *J. Appl. Phys.* **1959**, *30*, 1205.
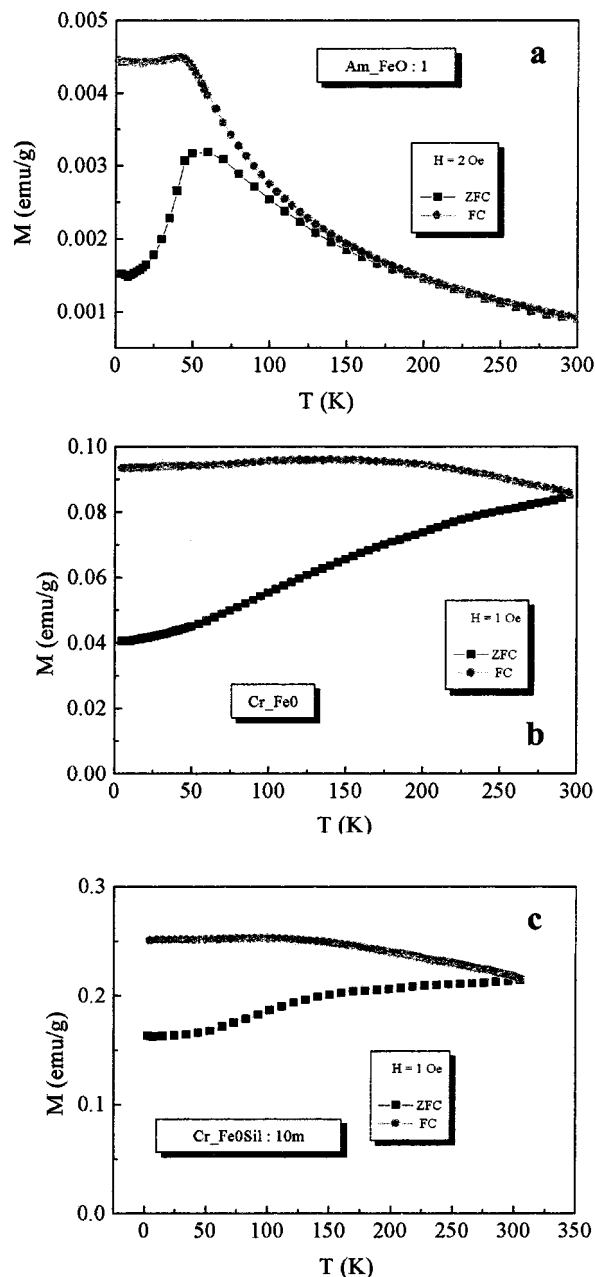

Figure 7. Field cooled (FC) and zero field cooled (ZFC) magnetization of as-prepared amorphous (a) (Am_FeO:1), crystalline uncoated (b) (Cr_FeO), and OTHS-coated (c) (Cr_FeOsil: 10 min) nanoparticles of γ-Fe₂O₃.

Oe) for coherent magnetization reversal of single domain, randomly oriented particles. This indicates that there is no contribution of shape anisotropy to total crystalline anisotropy and that no appreciable morphological change, either in size or shape, occurs during sonication with surfactant. The low values of remanence and coercivity are characteristic of soft ferromagnetic materials. Thus, the increased magnetization for the silane-coated particles is probably due to the increase in lattice ordering or high crystallinity compared to those of the uncoated one.

Field cooled (FC) and zero field cooled (ZFC) magnetization curves of the amorphous as-prepared, as well as crystalline, γ-Fe₂O₃ nanoparticles before and after coating with OTHS are shown in Figure 7. As expected, the amorphous as-prepared particles show a sharp
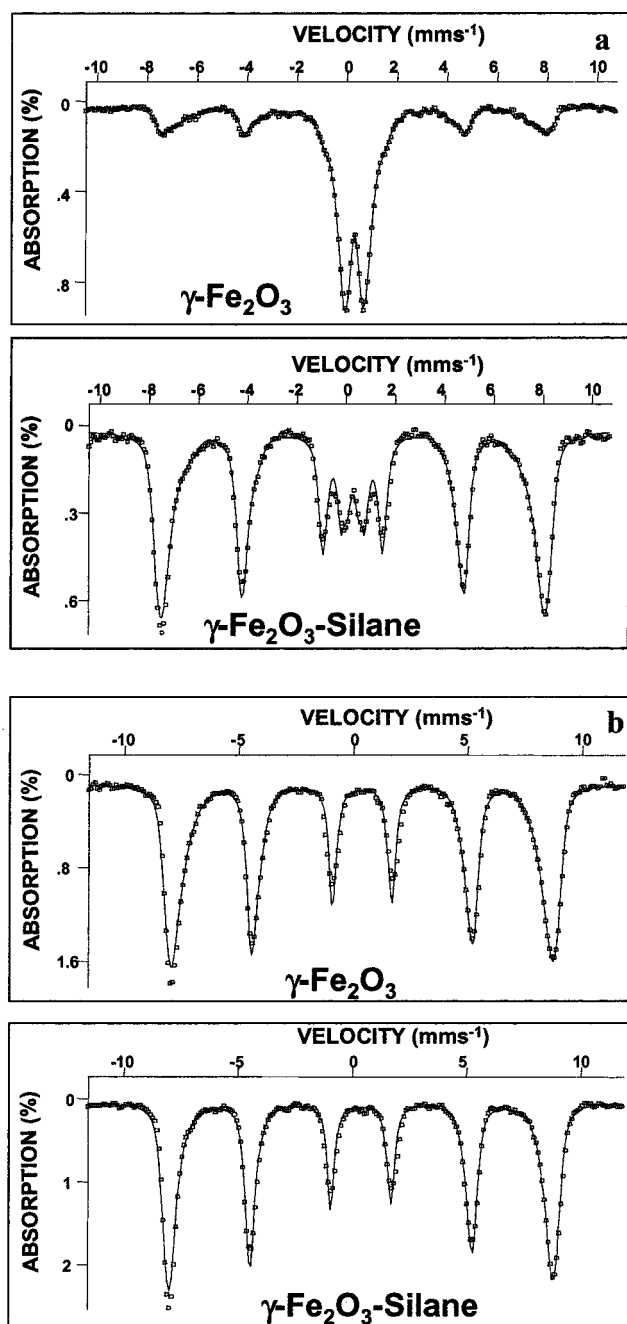
Figure 8. Mössbauer spectra of the crystalline and OTHS-coated nanoparticles of γ-Fe$_2$O$_3$ measured at 293 (a) and 4.2 K (b).

Table 1. Mössbauer Spectral Parameters for Cry–Fe$_2$O$_3$ and Cry–Fe$_2$O$_3$–Silane at 4.2 and 298 K[a]

			$T = 4.2$ K		
sample	DIS	δ (mm·s^{-1})	ϵ (mm·s^{-1})	H^* (Tesla)	% population[b]
γ-Fe$_2$O$_3$	H1	0.44	−0.005	51.4 ± 0.5	80 ± 1
	H2	0.40	0.005	49.3 ± 0.5	20 ± 1
γ-Fe$_2$O$_3$ silane	H1	0.44	−0.005	52.4 ± 0.5	72 ± 1
	H2	0.40	0.005	50.6 ± 0.5	28 ± 1

			γ-Fe$_2$O$_3$, $T = 293$ K		
DIS	δ (mm·s^{-1})	ϵ (mm·s^{-1})	Δ^* (mm·s^{-1})	H^* (T)	% population[a]
H1	0.34	−0.005		51.4	28
H2	0.30	0.005		49.3	2
EQ1	0.36		0.99		48
EQ2	0.30		0.76		22

			γ-Fe$_2$O$_3$ Silane, $T = 293$ K		
DIS	δ (mm·s^{-1})	ϵ (mm·s^{-1})	Δ^* (mm·s^{-1})	H^* (T)	% population[a]
H1	0.34	−0.005		48.1	31
H2	0.30	0.005		47.4	55
EQ1	0.32		0.76		14

[a] δ is the isomer shift, ϵ is the perturbation of the electrical field, Δ^* is the average quadrupolar splitting, H^* is the average hyperfine field, and Γ is the line width fixed at the classical value ($\Gamma = 0.35$ mm·s^{-1}). [b] Refined parameters.

and c) of the crystalline nanoparticles show divergence, and no blocking temperature characteristic of superparamagnetic relaxation is observed below 300 K. The magnetic anisotropy is directly related to the spm relaxation, and the divergence of the FC and ZFC curves is the measure of superparamagnetism. Note that for coated particles the divergence is less when compared to that for the uncoated ones, showing the increased ferromagnetic order of the former.

Mössbauer spectra for γ-Fe$_2$O$_3$ nanoparticles, as dry powder, before and after coating with OTHS at 293 and 4.2 K are shown in Figure 8. The points represent experimental results, and the refined data are shown as a solid line. The parameters obtained are presented in Table 1.

The difference between the room-temperature and low-temperature isomer shifts is due to the thermal variation of the second-order Doppler effect.[11,33e] At 293 K (Figure 8a), only Fe^{3+} in an octahedral environment is present in both samples. Both spectra may be described as a mixture of a magnetic component (sextuplet more or less resolved) and a nonmagnetic component (superparamagnetic quadruple doublet). The magnetic component (sextuplet) is more prominent in the coated γ-Fe$_2$O$_3$ sample, suggesting more ordering. The γ-Fe$_2$O$_3$ sample is more superparamagnetic (70%) than its coated γ-Fe$_2$O$_3$ counterpart (14%). The high degree of superparamagnetic component in the uncoated sample is an indication of the presence of amorphous impurities. Because of the existence of a sextuplet, it can be affirmed that, at 4.2 K (Figure 8b), both samples are magnetically ordered. The refinements with respect to the distribution of the internal magnetic field confirmed that only Fe^{3+} in the octahedral environment is present in both samples, that no superparamagnetism is detected, and that the samples are identical (environment, behavior) and ferromagnetically ordered at this temperature. The Mössbauer parameters corresponding

maximum in ZFC curve (Figure 7a), which is characteristic of a spin-glass type material. The blocking temperature of the spm particle is 50 K, which is defined as the maximum in the ZFC curve.[39]

The broad nature of the susceptibility curve indicates the distribution of the particle size, and the irreversibility occurs below 150 K. The blocking temperature and measurement time constants are consistent with a magnetic particle diameter of 8 nm, assuming a typical uniaxial anisotropy of 10^5 J·m^{-3} and using the relation $KV = 25KT_{\text{B}}$, where K is the anisotropy constant, V is the volume of the magnetic particle, and T_{B} is the blocking temperature. ZFC and FC curves (Figure 7b

(39) Leslie-Pelecky, D. L.; Rieke, R. D. *Chem. Mater.* **1996**, *8*, 1770.

Magnetic Enhancement of γ-Fe₂O₃ Nanoparticles

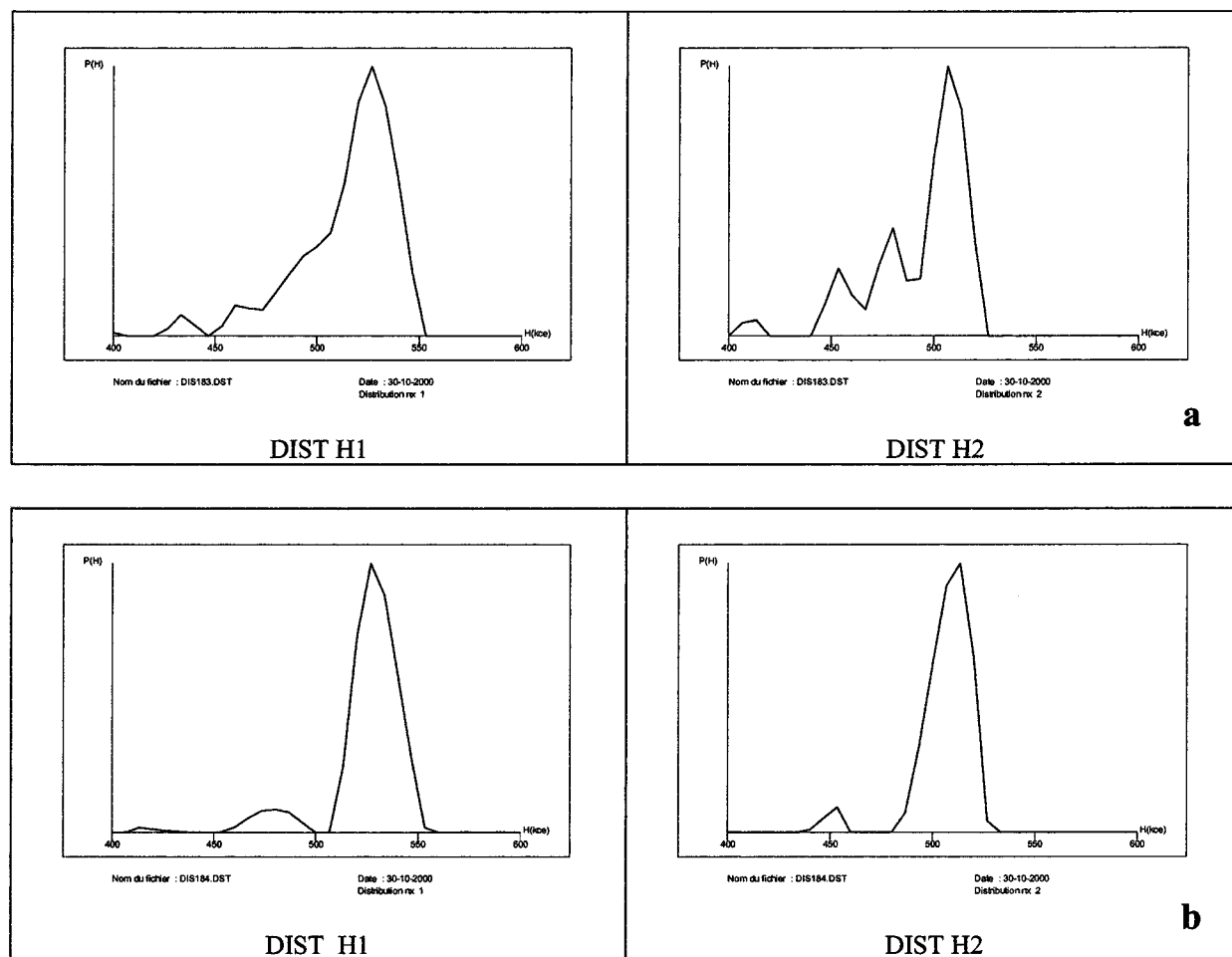*Chem. Mater., Vol. 14, No. 4, 2002* **1785**

Figure 9. Hyperfine field distributions obtained for Cr_FeO at $T = 4.2$ K (a) and for Cr_FeOSil: 10 min at $T = 4.2$ K (b).

to Fe^{3+} in octahedral sites are the same for both coated and uncoated nanoparticles. Thus, no change in the local environment of the Fe^{3+} ion occurs upon coating. The observed hyperfine field value is lower than that for bulk maghemite (about 52.6 T at 4 K), because, for nanoparticles and thin films, a reduced value is normally observed.[20,33e] Notice that the mean hyperfine field value H_{eff} is larger for the coated nanoparticles than the uncoated counterparts and it almost approached the bulk value. Calculations suggest that the before-coating γ-Fe_2O_3 sample is more disordered than the OTHS-coated counterpart, that is, that it shows inhomogeneity in the hyperfine field distribution, with the distribution more important with some values at low fields (Figure 9).

The inverse spinel structure of γ-Fe_2O_3 is known to have cation vacancies leading to superstructures: an ordered distribution with tetragonal symmetry (space group $P4_32_12$), resulting in partially ordered cubic superstructure (space group $P4_132$), or a random distribution (space group $Fd3m$).[36] Thus, because of internal disorder, the core magnetic moments can be canted, leading to the observed decrease in magnetization, and slightly different hyperfine field values of the iron atoms in the two sites A and B are possible. Morales and co-workers have observed a hyperfine field of 51.0 ± 0.5 T for the A site (tetrahedral) and 52.6 ± 0.3 T for the B site (octahedral) at 80 K.[36]

To further investigate the magnetic behavior of the OTHS-coated Fe_2O_3 nanoparticles, we carried out de-

tailed electron paramagnetic resonance (EPR) studies. Amorphous, as-prepared nanoparticles give a narrow resonance line ($\Delta H_{pp} = 416$ G) with an effective g-value of 2.04, which is in good agreement with that reported for Fe_2O_3 oxide glass.[32,40] The spectrum of the Fe^{3+} coupled pair ($Fe^{3+}-O-Fe^{3+}$) in Fe_2O_3 gives a resonance line at $g_{eff} = 2.0$. The crystalline (heated) particles, both coated with OTHS and uncoated, show rather broad ($\Delta H_{pp} = 1200-1300$ G) resonance lines at room temperature (RT). Silane modification of Fe_2O_3 particles led to higher g-values (Figure 10a). The spin density of these samples is at the level of $\sim 5 \times 10^{22}$ spins/g of sample, corresponding to Fe^{3+} paramagnetic species, in agreement with Mössbauer results.

Upon cooling, a monotonic increase in the g-values (Figure 10a) and in the peak-to-peak line width (ΔH_{pp}, Figure 10b) is observed for all nanoparticles. The line width of the EPR spectra of these samples is observed in an approximately linear variation with temperature. The lower the temperature, the broader is the line width, and a line width of about $1800-2000$ G is reached at 140 K.

This is a typical behavior of superparamagnetic nanoparticles, whose direction of magnetization fluctuates at a rate faster than the Larmor frequency. This results in a narrow resonance line due to an averaging effect of the fluctuations on the magnetocrystalline

(40) Tanaka, K.; Kamiya, K.; Yoko, T.; Tanabe, S.; Hirao, K.; Soga, N. *J. Nano-Cryst. Solids* **1989**, *109*, 289.
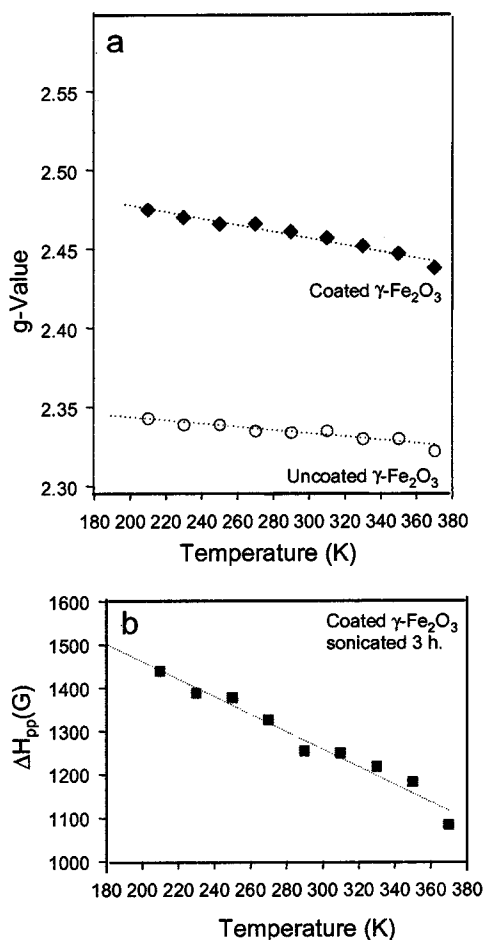
Figure 10. Temperature dependence of *g*-values for uncoated γ-Fe₂O₃ and for coated γ-Fe₂O₃ formed after 1 h of sonication with OTHS (a) and of ΔH_{pp} for coated γ-Fe₂O₃ nanoparticles formed after 3 h of sonication with OTHS (b).

anisotropy. On lowering the temperature, the resonance line of the superparamagnetic nanoparticles broadens as the averaging effect of thermal fluctuations is reduced and the direction of magnetization is blocked, at first in bigger, and progressively in smaller, particles. Other crystalline nanoparticles, such as the systems we investigated here, are also known to exhibit behavior like that of spin-glass materials, showing a broadening and a low-field shift of the EPR line width with a temperature decrease.[41] Magnetocrystalline anisotropy, in conjunction with the random orientations of the particles, causes line broadening in the ferromagnetic resonance (FMR) spectra of the monodomain ferromagnetic particles. The increased magnetic field produced by the magnetocrystalline anisotropy, as well as the strong interparticle interaction (dipolar) in our sample, is the reason for the increased *g*-value.[20,33a] As can be seen in TEM micrographs (Figure 1), the nanoparticles are highly aggregated, causing strong dipolar interactions.

(41) (a) Koksharov, Yu. A.; Gubin, S. P.; Kosobudsky, I. D.; Beltran, M.; Khodorkovsky, Y.; Tishin, A. M. *J. Appl. Phys.* **2000**, *88*, 1587. (b) Malozemoff, Jamet; Malozemoff, A. P. *Phys. Rev. B* **1978**, *18*, 75. (c) Nagata, K.; Ishihara, A. *J. Magn. Magn. Mater.* **1992**, *104–107*, 1571. (d) Massart, R.; Zins, D.; Gendron, F.; Rivoir, M.; Mehta, R. V.; Upadhyay, R. V.; Goyal, P. S.; Aswal, V. K. *J. Magn. Magn. Mater.* **1999**, *201*, 73. (e) Koksharov, Yu. A.; Gubin, S P.; Kosobudsky, I. D.; Yurkov, G. Yu.; Pankratov, P. L. A.; Mikhev, M. G.; Beltran, M.; Khodorkovsky, Y.; Tishin, A. M. *Phys. Rev. B* **2000**, *63*, 12407.
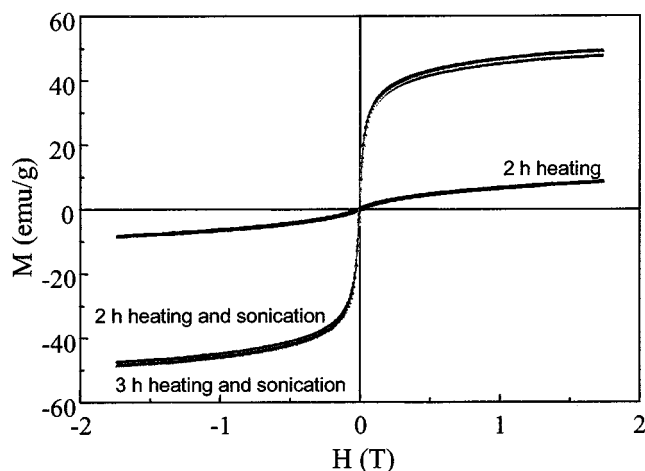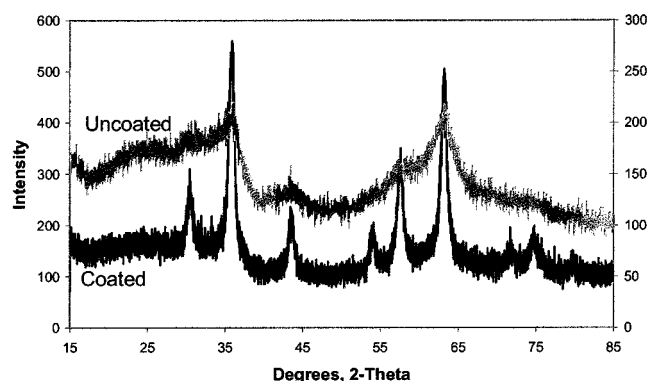

Figure 11. Room-temperature magnetization curves of the crystalline (heated at 300 °C for 2 h) and OTHS-coated (sonochemically for various periods of time) nanoparticles of γ-Fe₂O₃.

All these observations lead to the conclusion that the uncoated γ-Fe₂O₃ sample has more superparamagnetic nature than the coated sample, and the observed enhanced magnetization in the OTHS-coated γ-Fe₂O₃ nanoparticles is due to improved crystallinity.

This observation raised the question: What causes the ordering effect? This is not the sonication *per se*, since samples that were sonicated without the surfactant did not show an increase in either crystallinity or magnetization. In an attempt to answer this question, we coated amorphous Fe₂O₃ nanoparticles with OTHS after heating at 300 °C for different time periods. Figure 11 presents room-temperature magnetization curves of amorphous Fe₂O₃ nanoparticles after heating for 2 h at 300 °C before and after sonochemical coating with OTHS. Curves of samples heated for 3 h at 300 °C and coated with silane are included for comparison.

The small magnetization ($\sim$10 emu g^{-1}) of the sample before coating suggests that the nanoparticles are mostly amorphous. After sonochemical coating, the magnetization value increases tremendously ($\sim$50 emu g^{-1}), as observed for an amorphous sample heated at 300 °C for 3 h.

This is supported by XRD studies, as presented in Figure 12. The sample heated at 300 °C for 2 h and sonicated for 3 h in the pure solvent shows amorphous impurities, as the peaks are broad, whereas the sonochemically coated sample gives a clear crystalline pattern whose peak position and intensity match with reported JSPDS reference data for γ-Fe₂O₃. No trace of α-Fe₂O₃ (hematite) was detected in the sample.

When samples were heated for 4 h and more, at 300 °C, the magnetization values were almost the same for both coated and uncoated samples and show XRD features characteristic of highly crystalline nanoparticles with no amorphous impurities. This suggests that the particles have ordered during annealing, and no further ordering can be accomplished by sonochemical coating, further supporting the conclusion that sonochemical coating with OTHS results in increased crystallization and ordering of γ-Fe₂O₃ when nanoparticles contain amorphous impurities.

To further understand the relationship between magnetization enhancement and nanoparticle coating, we

Figure 12. XRD pattern for the uncoated Am_Fe₂O₃ nanoparticles after heating for 2 h at 300 °C, and the same sample analysis from TGA curves of γ-Fe₂O₃ crystalline nanoparticles, before and after coating with OTHS for various periods of time (10 ≤ *t* ≤ 180 min).

have coated γ-Fe₂O₃ nanoparticles heated at 300 °C for 4 h—from the same batch and with the same treatment history—with four different surfactants all having octadecyl chains ($C_{18}H_{37}SH$, $C_{18}H_{37}CO_2H$, $C_{18}H_{37}SO_3H$, $C_{18}H_{37}PO_3H_2$). While detailed results will be published in a forthcoming paper, preliminary studies revealed a marginal reduction in magnetization upon coating with the four surfactants.[42] Liu and co-workers[27] also observed a marginal reduction (2 emu/g) in saturation magnetization, 52.7 emu/g for a commercial crystalline γ-Fe₂O₃ sample (size 20 nm, purchased from Alpha) coated with mercaptohexadecanoic acid (MHA). Here, the reason for the reduction could be attributed to the diamagnetic contribution of the surfactant.

Thus, what we are left with is the chemical reaction of OTHS with the γ-Fe₂O₃ nanoparticles. Sonochemistry provides significant activation energy at the nanoparticle surface, and reactions that might otherwise not occur can take place. However, we believe that OTHS reaction with surface Fe−OH groups is not the origin of the magnetization enhancement, since other surfactants having the same chain length, when reacted with these groups, showed no enhancement. Therefore, the reaction of OTHS with the γ-Fe₂O₃ nanoparticles must result in the elimination of chemical impurities, the result of which is the removal of amorphous impurities and enhanced crystallization. Since SiH_3 is a reducing group, one possible reaction is with iron carbide that

might exist in sonochemically prepared γ-Fe₂O₃ nanoparticles (no stretching band for trapped CO was detected in the FTIR spectra of heated samples). If such a reaction occurs, impurities will be removed, allowing crystalline growth, which will reduce the amorphous component and increase magnetization. The enhanced magnetization can thus be accounted for by the removal of the magnetic dead layer.

Conclusions

Sonochemistry is an efficient and facile route for quantitative coating of γ-Fe₂O₃ nanoparticles with OTHS. The presence of C−H stretching (2950−2850 cm⁻¹) and bending (1475−1375 cm⁻¹) bands, and the absence of peaks at 2150 and 925 cm⁻¹(Si−H stretching and bending, respectively) confirm the presence of grafted hydrocarbon chains in the sonicated sample, hence the reaction of OTHS with γ-Fe₂O₃ nanoparticles. Ample evidence was presented suggesting that OTHS is a unique surfactant. The coated nanoparticles show increased magnetization (55 emu g⁻¹) compared to the uncoated ones (35 emu g⁻¹). XRD shows increased crystallinity after coating, compared to samples that were sonicated in the pure solvent. Mössbauer spectra reveal that the magnetic component (sextuplet) is more prominent in the OTHS-coated γ-Fe₂O₃ sample, suggesting more ordering. The γ-Fe₂O₃ sample is more superparamagnetic (70%) than its OTHS-coated γ-Fe₂O₃ counterpart (14%), indicating the presence of amorphous impurities in the former, which are removed in the OTHS coating process. EPR measurements reveal an increase in the *g*-value for the coated samples, suggesting increased magnetic ordering and crystallinity. Taken together, the experimental data presented confirm that the observed magnetization enhancement results from the reduction of chemical impurities by the SiH_3 group.

(42) Ansil, D.; Shafi, K. V. P. M.; Ulman, A.; Yan, X.; Yang, N.-L.; Estournes, C. In preparation.